J Mol Model (2013) 19:3333–3338
DOI 10.1007/s00894-013-1868-y

ORIGINAL PAPER

Electron-induced reductive debromination of 2,3,4-tribromodiphenyl ether: a computational study

Jin Luo · Jiwei Hu · Yuan Zhuang · Xionghui Wei · Xianfei Huang

Received: 4 February 2013 / Accepted: 23 April 2013 / Published online: 15 May 2013

Abstract To better understand the mechanism of the electron induced elimination of the bromide anion, we examined at the B3LYP/6-31+G(d) level electron capture by 2,3,4-tribromodiphenyl ether (BDE-21) followed by the release of the bromide anion and a radical. Both the geometry and energy of the BDE-21 neutral and its possible anionic states were studied. A significant relationship was found between the total energy and the length of the C-Br bonds by the analysis of the potential energy surface for the anionic states. Debromination preference for the bromine substituted positions was theoretically evaluated as meta-Br>ortho-Br>para-Br. The reaction profiles of the electron-induced debromination of BDE-21 demonstrated that, in general, the presence of a solvent makes the electron induced reductive debromination of BDE-21 significantly more advantageous, and the stabilization effect of the solvent on the reaction intermediates would make the electron attachment and dissociation relatively effective in comparison with the results from the gas-phase calculations.

Keywords Anions · Debromination · DFT · 2,3,4-Tribromodiphenyl Ether

Introduction

Polybrominated diphenyl ethers (PBDEs), which are used as additive flame retardants, have been widely detected in environmental and human samples [1–5]. PBDEs and their metabolites are in general persistent, bioaccumulative and structurally related to polychlorinated biphenyl (PCBs) and thyroid hormones, and their increasing levels in the environment pose a potential danger to human health *via* endocrine disruption, neurotoxicological effects, carcinogenicity, *etc.* [6–10]. Studies to date have showed that debromination of PBDEs could occur *via* multiple processes (*e.g.*, chemical [11–13], photochemical [14, 15] and biological processes [16, 17]). Recently, treatment using zero-valent iron (ZVI) to reduce PBDEs to less toxic products (*e.g.*, diphenyl ether) is considered to be a promising strategy for remediation of the PBDE contamination [11–13].

In the presence of ZVI, PBDEs can be debrominated rapidly to lower brominated congeners or diphenyl ether. Although the debromination rates of PBDEs by different-sized ZVI varied significantly, a satisfactory quantitative property-reactivity relationship has been observed between the specific surface area normalized reaction rates and lowest unoccupied molecular orbital energies, indicating the direct electron transfer as a major reaction mechanism between PBDEs and ZVI [12, 18–20]. In general, the presence of the highly electronegative bromine atom in the molecules can make their anions relatively stable. Several reports have suggested that PBDEs can accept electron and undergo a reductive dehalogenation due to its large positive electron

Electronic supplementary material The online version of this article (doi:10.1007/s00894-013-1868-y) contains supplementary material, which is available to authorized users.

J. Luo · J. Hu (✉) · X. Huang
Guizhou Provincial Key Laboratory for Information Systems of Mountainous Areas and Protection of Ecological Environment, Guizhou Normal University, Guiyang 550001, People's Republic of China
e-mail: jiweihu@yahoo.com

J. Hu
e-mail: jwhu@gznu.edu.cn

Y. Zhuang
Department of Civil and Environmental Engineering, Stanford University, Stanford, CA 94305, USA

X. Wei
Department of Applied Chemistry, College of Chemistry and Molecular Engineering, Peking University, Beijing 100871, People's Republic of China

affinity and relatively low energy of lowest unoccupied molecular orbital [11, 12, 18, 19]. Recently, density functional theory (DFT) calculations were carried out to study the structures of anions of halogenated aromatic compounds (*e.g.*, polychlorinated dibenzo-p-dioxins [21, 22], polychlorinated dibenzofurans [23] and PBDEs [24, 25]). It was found that the equilibrium nuclear configuration of the anion might correspond to some point along the pathway to dissociation of the neutral molecule. Considerable elongation (by 0.6–0.8 Å approximately) of a specific carbon-halogen bond was observed in most of the optimized structures, indicating that the added electron clearly weakens the carbon-halogen bond and makes it more vulnerable to dissociation [25, 26]. For PBDEs, the substituted position where the considerable elongation of C–Br bond occurs in theoretical calculations can be viewed as the vulnerable dehalogenation position, where the reductive debromination was somehow observed experimentally in the reaction with ZVI [12, 25] or on electron capture negative ion mass spectrometry [22]. In this regard, upon accepting an electron, the geometrical changes in PBDE congeners may provide fundamental information for the understanding of debromination sites and processes. In the reaction of PBDEs with ZVI, meta- was found to be the most susceptible substituted position for the cleavage of the C–Br bond to occur, however, the products from the para- and ortho-debromination of parent compounds could also be observed [12, 18].

To better understand the electron acceptance (reduction) and carbon-bromine bond cleavage mechanisms of PBDEs and their debromination regioselectivity, 2,3,4-tribromodiphenyl ether (BDE-21) having one bromine at each of the ortho-, meta-, and para- positions on one side of diphenyl ether was selected in this paper for a computational study. We report herein the DFT calculations that address: (1) the characteristics of the radical anions formed after an electron transferred to BDE-21 neutral, (2) relative stabilities of the possible BDE-21 anionic states and the transition states for their isomerization, and (3) reaction profiles for the electron-induced dissociation of BDE-21.

Computational methods

All calculations in the present research were performed with Gaussian03 [27], and GaussView 4.1 was used as the molecular modeling system for constructing and visualizing the results of the calculations. The split valence 6-31+G(d) basis set [28], including the minimum addition of diffuse functions, in combination with the hybrid density functional Becke3LYP [29, 30], was chosen for the geometry optimization, frequency and energy calculations, since the B3LYP/6-31+G(d) calculation was previously reported in good agreement with the experimental electron attachment energy for several BDEs (by means of electron transmission spectroscopy and dissociative electron attachment spectroscopy) [31] and the basis set effects are not obvious on the geometrical structure for BDE-21 according to our earlier report [25]. Effects of the solvent were included through single-point calculations at the same level of theory using the conductor polarized continuum model (CPCM) [32]. To mimic the situation in mixtures of acetone (ε=20.7) and water (ε=78.4) (1:1) used in the previous BDE-21 debromination experiment [12], the dielectric constant in the present work was set to ε=32.63 (methanol) [32]. Discussions in this study were primarily based on the calculations in solution if not noted, and the detailed thermodynamic data in the gas-phase (Table A.1) and in solution (Table A.2) can be found in Appendix.

Results and discussion

Molecular geometry of BDE-21

Presently, no structural data based on the X-ray diffraction are available for BDE-21, however, the reliability of the geometric data calculated at the B3LYP/6-31+G(d) level for BDE homologues have been validated by previous researchers [24, 25]. According to the earlier reports [24, 25], the discrepancies were slight between the experimental and theoretical geometries. The geometric parameters of the BDE-21 neutral and its possible anionic states obtained from optimizations in this study are shown in Fig. 1, and the Cartesian coordinates for the optimized structures from our calculations can be found in Appendix.

It was found that geometries of the three BDE-21 anionic states (**I**, **II** and **III**) are significantly different from that of the neutral species. For the BDE-21 neutral, the calculated C-Br bond lengths varied from 1.883 Å (the ortho-position) to 1.895 Å (the para-position), increasing with the distance of substitution position from the O atom. For the anionic states, all C-Br bonds were elongated as compared to those of the BDE-21 neutral at the corresponding brominated position. When the electron was added, one particular C–Br bond was lengthened from around 1.89 Å (in the neutral BDE-21) to around 2.4 Å (in the anionic states). It was reported that debromination of PBDEs might occur as the departing bromine bent off the aromatic ring plane for effective π*-σ* orbital mixing [24, 25]. In the present study, bending of the C–Br bond out of the aromatic ring plane was only observed at the ortho-position of anionic state **I**. In addition, another geometrical change observed in BDE-21 anionic states involved a transformation in the torsion angles to lower the total energy. The conformation was changed from a skew type in the BDE-21 neutral to a twist in BDE-

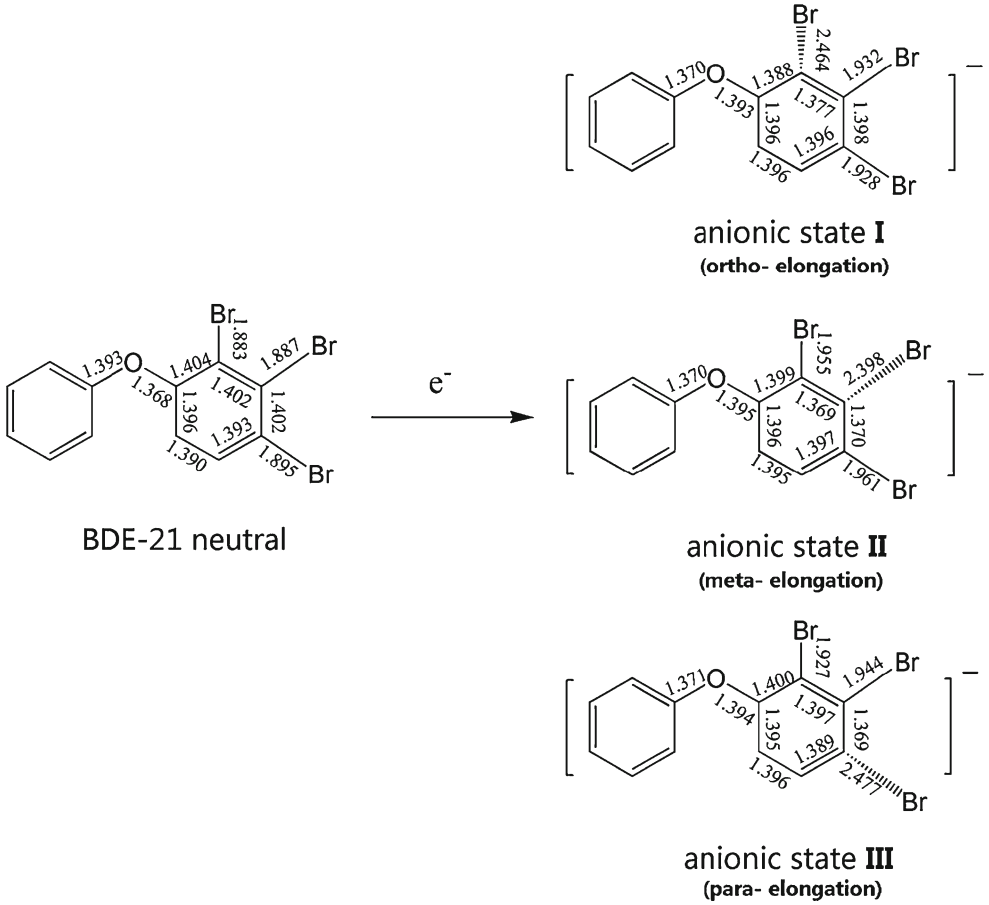

Fig. 1 Structure and some important geometrical parameters of BDE-21 and its possible radical anionic states obtained from the B3LYP/6-31+G(d) calculations (bond distances are given in angstroms)

21 anions [33], thus the unsubstituted aromatic ring plane turned out to be closer to the bromine atom, benefiting from a stabilization of the added electron. The large positive electron affinity values calculated in the present research (Table 1) are in support of the notion that PBDEs could act as electron acceptors in the charge-transfer interaction with reductants such as ZVI [12] and birnessite [34]. These anionic states might be more appropriate to be considered as a species with an extended three-electron C-Br bond since the bromine carried some of the unpaired spin density (Fig. 2) and not a full negative charge (around −0.5e in this study) [32].

Anionic states and the possible bromide ion loss channel for BDE-21

The equilibrium nuclear configuration of the radical anion should correspond to some point along the pathway to the dissociation. Electron attachment to neutral BDE-21 could elongate the C-Br bond. When the change occurs on the potential energy surface of the anion, the neutral-anion energy separation will decrease, following the relaxation of the nuclear configuration. It was found that the geometry optimization of BDE-21 obtained through vertical electron transfer (electron attached to the neutral without a geometry change) to the structure of the neutral molecule led directly to anionic state **II**, as was observed in our previous report [25]. The preferred formation of anionic state **II** over alternative anionic state **I** or anionic state **III**, may be a reflection of the next lowest unoccupied molecular orbital (NLUMO) structure of the BDE-21 neutral [32]. The lowest unoccupied molecular orbital (LUMO) for the BDE-21 neutral (orbital 97) is almost completely located on the brominated phenyl group, and concentrated on the three C-Br bond especially, as shown in Fig. 2. From orbitals 97 to 101 (LUMO to LUMO+4), the spatial distribution of orbital densities is gradually moved to the unsubstituted phenyl group and the orbital character changed from σ* to π* (shapes of the molecular orbitals do not vary significantly between calculations in the gas-phase and in solution).

In the electron induced debromination of some brominated nucleobases [35], conversion of the nuclear configuration of the neutral to its anionic species is associated with a small kinetic barrier. In the present research, this conversion process for BDE-21 was found to be barrier-free. We have drawn the potential energy surface by rigid scan along the two C-Br bonds of the anionic BDE-21, as shown in Fig. A.1. The shallow-type minima, which may behave as a temporary dissociative state, were found with a suitable length (around 2.4 Å) for each C-Br bond at the

Table 1 Thermodynamic characteristics of each step as well as the global (ΔE) driving force for the electron-induced release of the bromide anion from BDE-21 (kJ mol^{-1})

	In the gas-phase				In solution			
	Step 1	Step 2	Step 3	Global	Step 1	Step 2	Step 3	Global
Sate I	−26.32	−69.12	103.34	7.90	−172.42	−99.62	9.83	−262.21
Sate II	−26.32	−65.94	100.88	8.62	−172.42	−101.04	12.84	−260.62
Sate III	−26.32	−60.08	98.91	12.51	−172.42	−94.52	9.12	−257.82

corresponding substituted position of the BDE-21 anion. It was found that energy of the molecule decreased significantly with the increase in the C-Br bond length. The elongation of one specific C-Br bond is reasonable for the BDE-21 anion. When the vertical electron transfer occurred to BDE-21, either the fixing or elongation of all the C-Br bonds would cause a rise in energy.

In this study, to elucidate the possible bromide ion loss channels, isomerization between possible anionic states were investigated by transition state theory calculations. The obtained geometries of transition states are similar to the equilibrium structure of BDE-21 anions, but have two obviously elongated C-Br bonds with the stretching vibration showing an imaginary frequency. In the gas-phase, the energy order of three anionic states was **I**<**II**<**III**, with the relative energy of 0, 3.18 and 9.04 kJ mol^{-1}, respectively. However, in solution, state **II** is the relatively stable species, followed by anionic **I** (1.43 kJ mol^{-1} higher) and anionic **III** (6.52 kJ mol^{-1} higher). The dominant bromine loss channel (meta-) represented by the relatively stable species (anionic state **II**) in solution phase calculation was also observed experimentally in a recent report on the reductive debromination of BDE-21 by ZVI in acetone/water solution (1:1) [12]. Figure 3 shows the relative energy diagram of the anionic states **I**, **II** and **III**, and the transition states between them. Isomerization of state **II** to **I** and **III** is possible by breaking the conversion barrier around 20 kJ mol^{-1}. This low conversion barrier energy indicated that debromination of BDE-21 can occur at either the meta-, ortho- or para-position, as was observed experimentally [12]. The debromination preference for the substituted position in solution is theoretically evaluated as the meta-Br>ortho-Br >para-Br, being in good agreement with previous experimental debromination using ZVI and theoretical calculation [12, 18, 25]. However in the gas-phase, the debromination preference based on the energy of anionic states is ortho-Br >meta-Br>para-Br. In addition, the transition state, with two considerably elongated C-Br bonds, might be unstable and could easily lose its bromide anion as the dissociation occurred at the elongated C-Br bond in anionic states. This could probably explain the presence of mono-BDEs in the experimental debromination of individual BDE-21 [12],

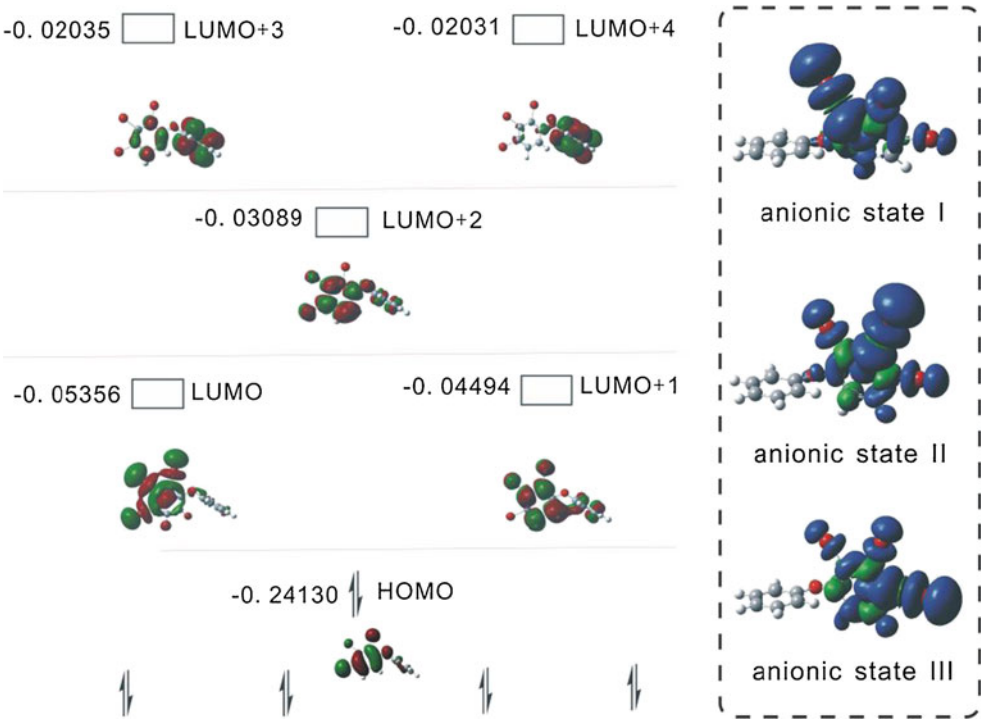

Fig. 2 Orbital energy (hartree), HOMO, LUMO, NLUMO (left, iso-surface value=0.02 au, degeneracy threshold = 0.01 hartree) and spin density (right, iso-surface value= 0.0004 au) surface image (in solution)

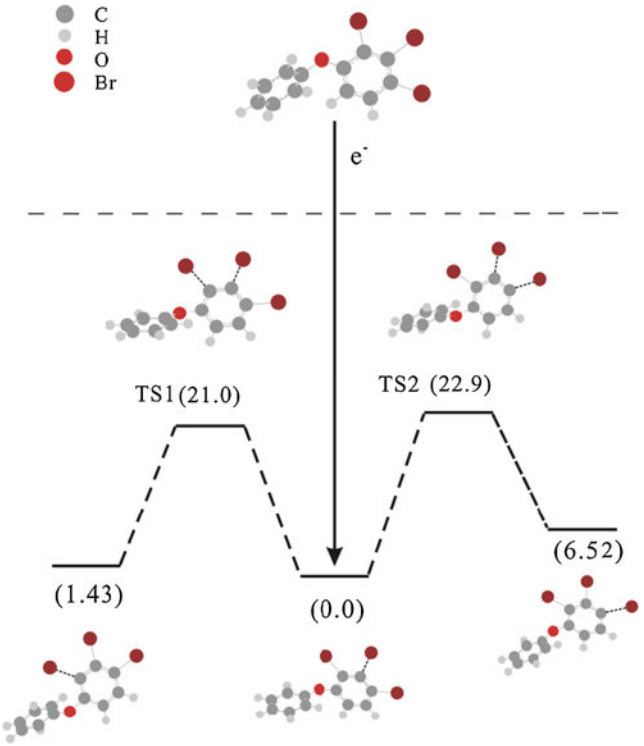

Fig. 3 Relative energy diagram (in solution) of the anionic states I, II and III, and the transition states between them (kJ mol^{-1})

which is generally considered to be a stepwise and sequential reaction. Since a certain amount of unknown byproducts was observed experimentally [12], other pathways might also exist in the debromination of BDE-21 and thus further research needs to be carried out in this field.

Reaction profiles for the electron-induced dissociation

The mechanism of C-Br bond breakage following electron attachment in BDE-21 can be divided into three steps (1) electron binding to the neutral BDE congener; (2) conversion of the electron adduct into the multiple anionic states; (3) complete separation of the Br^- anion and neutral radical molecule. The reaction profiles on the electronic energy scale are shown in Fig. 4 and Table 1.

In the present work, the energy change for this reaction indicated that formation of the radical anions from the BDE-21 neutral is thermodynamically feasible. In each step, the difference was small in energy of the reaction concerning the three anionic states. It was demonstrated computationally that, in general, the presence of the solvent makes the electron induced reductive debromination of BDE-21 significantly more advantageous than in the gas-phase. The most striking dissimilarities between the processes occurring in both the gas-phase and solution relate to steps 1 and 3. In solution, the vertical electron attachment energy (negative values of the energy in step 1) was up to 172.42 kJ mol^{-1}, whereas in the gas-phase, it was only 26.32 kJ mol^{-1}. Although the energies in step 1 for BDE-21 were all negative in our calculations, it is clear that stabilization effect of the solvent on the BDE-21 anions could make the vertical electron attachment process quite effective. For anionic states **I**, **II** and **III** in the gas-phase, the respective energies of step 2 were calculated to be −69.12, -65.94 and −60.08 kJ mol^{-1}, and the presence of the solvent makes this step slightly easier, with the energies of −99.62,−101.04 and −94.52, respectively. In step 3, the anionic state dissociation is significantly endothermic in the gas-phase, suggesting that thermodynamics might prevent BDE-21 anion separation into the bromide anion and the corresponding radical. However, owing to the solvation, this dissociation step was found accompanied by only a small energy barrier (around 10 kJ mol^{-1}), which would probably be easily overcome during the course of dissociation.

Conclusions

In the present research, the BDE-21 neutral and its radical anions were investigated at the DFT level. The positive electron affinities confirm the vertical and adiabatic stability of the anionic states in both the gas-phase and solution. The shallow-type minima were found in the potential energy surface by rigid scan of the C-Br bonds, which may behave as a temporary dissociative state. It was found that the geometry optimization of BDE-21 obtained through vertical

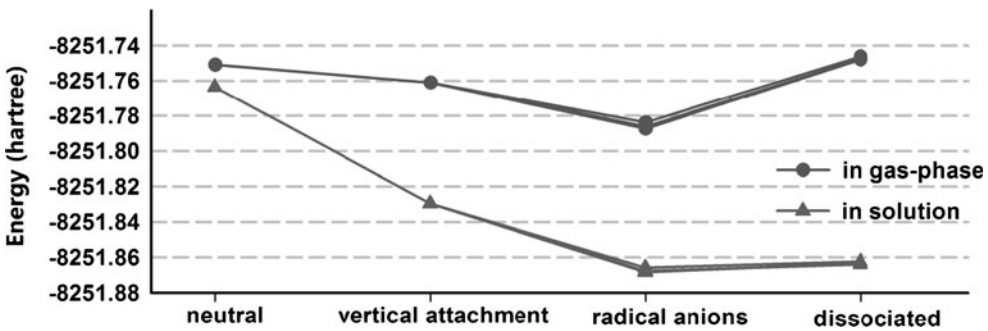

Fig. 4 Reaction profiles for electron-induced debromination of BDE-21 into the separated bromide anion and radical

electron transfer to the structure of the neutral molecule led directly to anionic state **II**, which can be transformed into states **I** and **III** through the transition states. Debromination preference for the substituted position in solution is theoretically evaluated as meta-Br>ortho-Br>para-Br, being in agreement with previous experimental results and theoretical calculation [12, 18, 25]. The reaction profiles of the electron-induced debromination of BDE-21 demonstrate that, in general, the presence of a solvent makes the electron induced reductive debromination of BDE-21 significantly more advantageous. The most striking dissimilarities between the debromination processes of BDE-21 occurring in the gas-phase and solution relate to vertical electron attachment and the bromide anion dissociation.

Acknowledgments This work was supported by the research funding from Guizhou Normal University, China.

References

1. Crimmins BS, Pagano JJ, Xia X, Hopke PK, Milligan MS, Holsen TM (2012) Environ Sci Technol 46:9890–9897
2. Rotander A, van Bavel B, Polder A, Rigét F, Auðunsson GA, Gabrielsen GW, Víkingsson G, Bloch D, Dam M (2012) Environ Int 40:102–109
3. Zhang K, Schnoor JL, Zeng EY (2012) Environ Sci Technol 46:10861–10867
4. Sjödin A, Patterson DG Jr, Bergman A (2003) Environ Int 29:829–839
5. Costa LG, Giordano G, Tagliaferri S, Caglieri A, Mutti A (2008) Acta Biomed 79:172–183
6. Legler J (2008) Chemosphere 73:216–222
7. Costa1 LG, Giordano G (2007) Neurotoxicology 28:1047–1067
8. Eriksson P, Jakobsson E, Fredriksson A (2001) Env Health Persp 109:903–908
9. Dingemans MML, van den Berg M, Westerink RHS (2011) Environ Health Perspect 119:900–907
10. Hu JW, Eriksson L, Bergman Å, Jakobsson E, Kolehmainen E, Knuutinen J, Suontamo R, Wei XH (2005) Chemosphere 59:1043–1057
11. Yu K, Gu C, Boyd SA, Liu C, Sun C, Teppen BJ, Li H (2012) Environ Sci Technol 46:8969–8975
12. Zhuang Y, Ahn S, Luthy RG (2010) Environ Sci Technol 44:8236–8242
13. Shih Y, Tai Y (2010) Chemosphere 78:1200–1206
14. Eriksson J, Green N, Marsh G, Bergman A (2004) Environ Sci Technol 38:3119–3125
15. Bezares-Cruz J, Jafvert CT, Hua I (2004) Environ Sci Technol 38:4149–4156
16. He J, Robrock KR, Alvarez-Cohen L (2006) Environ Sci Technol 40:4429–4434
17. Gerecke AC, Hartmann PC, Heeb NV, Kohler HP, Giger W, Schmid P, Zennegg M, Kohler M (2005) Environ Sci Technol 39:1078–1083
18. Keum Y, Li QX (2005) Environ Sci Technol 39:2280–2286
19. Zhuang Y, Ahn S, Seyfferth AL, Masue-Slowey Y, Fendorf S, Luthy RG (2011) Environ Sci Technol 45:4896–4903
20. Zeng X, Simonich SLM, Robrock KR, Korytar P, Alvarez-Cohen L, Barofsky DF (2010) Environ Toxicol Chem 29:770–778
21. Borisov YA, Garrett BC, Mazunov V, Nekrasov YS (2005) J Struct Chem 46:591–595
22. Zhao YY, Tao FM, Zeng EY (2007) J Phys Chem A 111:11638–11644
23. Arulmozhiraja S, Morita M (2004) J Phys Chem A 108:3499–3508
24. Zhao YY, Tao FM, Zeng EY (2008) Chemosphere 70:901–907
25. Hu JW, Zhuang Y, Luo J, Wei XH, Huang XF (2012) Int J Mol Sci 13:9332–9342
26. Luo J, Hu JW, Zhuang Y, Wei XH, Huang XF (2013) Chemosphere 91:765–770
27. Frisch MJ, Trucks GW, Schlegel HB, Scuseria GE, Robb MA, Cheeseman JR, Montgomery JA Jr, Vreven T, Kudin KN, Burant JC, Millam JM, Iyengar SS, Tomasi J, Barone V, Mennucci B, Cossi M, Scalmani G, Rega N, Petersson GA, Nakatsuji H, Hada M, Ehara M, Toyota K, Fukuda R, Hasegawa J, Ishida M, Nakajima T, Honda Y, Kitao O, Nakai H, Klene M, Li X, Knox JE, Hratchian HP, Cross JB, Adamo C, Jaramillo J, Gomperts R, Stratmann RE, Yazyev O, Austin AJ, Cammi R, Pomelli C, Ochterski JW, Ayala PY, Morokuma K, Voth GA, Salvador P, Dannenberg JJ, Zakrzewski VG, Dapprich S, Daniels AD, Strain MC, Farkas O, Malick DK, Rabuck AD, Raghavachari K, Foresman JB, Ortiz JV, Cui Q, Baboul AG, Clifford S, Cioslowski J, Stefanov BB, Liu G, Liashenko A, Piskorz P, Komaromi I, Martin RL, Fox DJ, Keith T, Al-Laham MA, Peng CY, Nanayakkara A, Challacombe M, Gill PMW, Johnson B, Chen W, Wong MW, Gonzalez C, Pople JA (2003) Gaussian 03. Gaussian Inc, Wallingford, CT
28. Hehre WJ, Ditchfield R, Pople A (1972) J Chem Phys 56:2257
29. Becke AD (1993) J Chem Phys 98:5648–5652
30. Lee C, Yang W, Parr RG (1988) Phys Rev B 37:785–789
31. Pshenichnyuk SA, Lomakina GS, Modellibc A (2011) Phys Chem Chem Phys 13:9293–9300
32. Nonnenberg C, van der Donk WA, Zipse H (2002) J Phys Chem A 106:8708–8715
33. Hu JW, Eriksson L, Bergman Å, Jakobsson E, Kolehmainen E, Knuutinen J, Suontamo R, Wei XH (2005) Chemosphere 59:1033–1041
34. Ahn MY, Filley TR, Jafvert CT, Nies L, Hua I (2006) Chemosphere 64:1801–1807
35. Chomicz L, Rak J, Storoniak P (2012) J Phys Chem B 116:5612–5619